Size-Controlled Production of Gold Bionanoparticles Using the Extremely Acidophilic Fe(III)-Reducing Bacterium, Acidocella aromatica

Intan Nurul Rizki
Department of Earth Resources Engineering, Faculty of Engineering, Kyushu University

Okibe, Naoko
Department of Earth Resources Engineering, Faculty of Engineering, Kyushu University

Size-Controlled Production of Gold Bionanoparticles Using the Extremely Acidophilic Fe(III)-Reducing Bacterium, *Acidocella aromatica*

Intan Nurul Rizki and Naoko Okibe *

Department of Earth Resources Engineering, Faculty of Engineering, Kyushu University, 744 Motooka, Nishi-ku, Fukuoka 819-0395, Japan; intan@mine.kyushu-u.ac.jp

* Correspondence: okibe@mine.kyushu-u.ac.jp; Tel.: +81-92-802-3312

Abstract: Recycling of gold-bearing "urban mine" resources, such as waste printed circuit boards (PCBs), is attracting an increasing interest. Some of the gold leaching techniques utilize acidic lixiviants and in order to eventually target such acidic leachates, the utility of the acidophilic Fe(III)-reducing heterotrophic bacterium, *Acidocella* (*Ac.*) *aromatica* PFBC was evaluated for production of Au(0) bionanoparticles (bio-AuNPs). Au(III) ions (as $AuCl_4^-$, initially 10 mg/L), were readily adsorbed onto the slightly-positively charged *Ac. aromatica* cell surface and transported into cytoplasm to successfully form intracellular bio-AuNPs in a simple one-step microbiological reaction. Generally, increasing the initial concentration of formate as e-donor corresponded to faster Au(III) bioreduction and a greater number of Au(0) nucleation sites with less crystal growth within 40–60 h: i.e., use of 1, 5, 10, or 20 mM formate led to production of bio-AuNPs of 48, 24, 13, or 12 nm in mean particle size with 2.3, 17, 62, and 97 particles/cell, respectively. Addition of Cu^{2+} as an enzymatic inhibitor significantly decreased the number of Au(0) nucleation sites but enhanced crystal growth of individual particles. As a result, the manipulation of the e-donor concentration combined with an enzyme inhibitor enabled the 3-grade size-control of bio-AuNPs (nearly within a normal distribution) at 48, 26 or 13 nm by use of 1 mM formate, 20 mM formate ($+Cu^{2+}$) or 10 mM formate, respectively, from highly acidic, dilute Au(III) solutions.

Keywords: gold nanoparticles; *Acidocella aromatica* PFBC; Fe(III)-reducing bacterium; acidophilic microorganism; size-control

1. Introduction

Industrial demands for precious-group metals (PGMs), together with the growing needs for cost effectiveness and implementation of green technology are increasing rapidly. Due to the rarity of the metals and their uneven distribution, the importance to recycle PGMs from secondary resources is inevitable. As one of the PGMs, Au is recognized as one of the most expensive metals historically in the world [1].

Today, industrial demands prefer Au mostly in the form of nanoparticles, rather than in bulk metal, owing to a variety of their unique properties. Nanoparticles tend to be more reactive due to their greater specific surface area than larger particles. Au(0) nanoparticles (AuNPs) have thus been applied to many different applications across the field of biology and medicine (e.g., labeling, bio-imaging, drug delivery [2,3]), environment (e.g., pollution control and water purification [4], catalysts for green chemistry [5,6], nanobiosensors in food and agriculture industry [7,8]), and technology (e.g., improving computer memory [9]).

A number of chemical synthesis methods have been so far reported for the production of AuNPs [10]. One of the most frequently used approaches is the in-situ chemical reduction method,

which consists of two major steps (i.e., the first chemical reduction step using agents, such as borohydrides, and the second stabilization step using agents, such as trisodium citrate dehydrate) [10].

For "greener" syntheses of AuNPs as compared to the conventional approaches, the usefulness of biological methods has recently been increasingly recognized. In these methods, a variety of biomaterials (such as plants, natural source extracts, chitosan, and microbial cells) directly act as both reducing agent and stabilizer to form AuNPs [10–13].

Among such biomaterials, bacterial cells are generally easily replicated and maintained, making them one of the most ideal low-cost materials for metal nanoparticles production. Since interactions between bacterial cells and different metals have been well documented [14], such natural geomicrobiological reactions have a great potential to be utilized in the production of diverse metal nanoparticles.

So far, studies on bacterial bio-AuNPs reported formations of a diverse size range of particles in different cellular locations (extra- and intracellular regions, including cell surface, periplasmic space and cytoplasms). These studies used either Au(I)-thiosulfate or Au(III)-chloride as a starting Au solution with or without e-donor, by employing extensively neutrophilic bacteria (even under acidic experimental pHs): i.e., different *Bacillus* spp. (a few nano- to micro-size, extra- and intracellular [15–20]); *Lactobacillus* spp. (5–30 nm, intracellular [21]; 20–50 nm and >100 nm, extra- and intracellular [22]); *Pseudomonas aeruginosa* (15–30 nm, extracellular [23]); *Escherichia coli* and *Desulfovibrio desulfuricans* (20–50 nm, intracellular; [24]); a range of dissimilatory Fe(III)-reducing bacteria/archaea including *Pyrobaculum islandicum*, *Pyrococcus furiosus*, *Thermotoga maritima*, *Shewanella algae*, *Geobacter sulfurreducens* and *Geovibrio ferrireducens* (nano-size, intracellular [25,26]); *Rhodopseudomonas capsulate* (10–20 nm, extracellular [27]); *Rhodobacter capsulatus* (<50 nm, extra- and intracellular [28]), *Stenotrophomonas maltophilia* (40 nm, intracellular [29]), *Ralstonia metallidurans* (extra- and intracellular [30]), sulfate-reducing bacteria (mostly <10 nm, extra- and intracellular [31]), and the radiation-resistant *Deinococcus radiodurans* (44 nm, extra- and intracellular [32]).

Since some of the gold leaching techniques utilize acidic lixiviants, such as chloride solution and thiourea, plus ferric iron solution, investigating the potential of extremely acidophilic bacteria for bio-AuNPs production is important. However, to our knowledge, the only acidophilic extremophile so far tested for bio-AuNPs production is the autotrophic S-oxidizer, *Acidithiobacillus (At) thiooxidans*. The bacterium deposited fine-grained Au(0) colloids (5–10 nm), by utilizing $Au(S_2O_3)_2{}^{3-}$ as an energy source, throughout the cell, especially along the cytoplasmic membrane [33].

In both neutrophilic and acidophilic bacterial AuNPs studies, as described above, attempts to control the particle size have been hardly reported.

Hence, the objective of this study was set to investigate the utility of the acidophilic Fe(III)-reducing heterotrophic bacterium, *Acidocella aromatica* PFBC, for the production of bio-AuNPs from acidic, dilute Au(III) solutions, especially with the aim to recover them with size-control.

2. Materials and Methods

2.1. Microorganism

Acidocella aromatica PFBC[T] (DSM 27026; [34]) was routinely maintained and pre-grown aerobically in 500 mL Erlenmeyer flasks containing 200 mL heterotrophic basal salts (HBS) medium (pH 2.5 with H_2SO_4; per liter; 50 mg KCl, 500 mg $MgSO_4 \cdot 7H_2O$, 50 mg KH_2PO_4, 450 mg $(NH_4)_2SO_4$, 142 mg Na_2SO_4, 14 mg $Ca(NO_3)_2 \cdot 4H_2O$) containing 10 mM fructose and 0.025% (*v/v*) tryptone soya broth (TSB). Flasks were incubated at 30 °C, and shaken at 100 rpm.

2.2. Bioreduction of Au(III) by Ac. aromatica Cell-Suspensions

Ac. aromatica was pre-grown aerobically, harvested at the late-exponential phase by centrifugation, washed twice, and finally re-suspended (to a final cell density of 10^9 cells/mL) in 25 mL of fresh HBS medium (pH 2.5; in 25 mL vials) containing 10 mg/L Au(III) (as $HAuCl_4 \cdot 3H_2O$). After incubating vials

for 1 h to allow Au(III) biosorption, sodium formate (HCOONa) was added as e-donor at 1, 5, 10, and 20 mM (It should be noted that sodium formate (pK_a = 3.75) added to the media hereafter was likely present predominantly as formic acid under the acidic conditions used.

Where indicated, Cu^{2+} (as $CuSO_4 \cdot 7H_2O$) was added to the medium at the initial concentration of 5 mM as a potential enzyme inhibitor at 1 h. Cell-free controls were also set up in parallel.

After cells were pre-grown aerobically, all of the solutions used were prepared anaerobically by N_2-purging (6 h/L-medium). Vials were sealed with butyl-rubber stoppers and aluminum crimps, and were incubated unshaken at 30 °C (in contrast, aerobic incubation did not reduce gold; data not shown).

Samples were regularly withdrawn and filtered (0.2 μm) to measure the total soluble Au concentration by ICP-OES (Perkin Elmer Optima 8300, Waltham, MA, USA). Following the completion of Au(III) reduction (using 20 mM formate), cells were harvested at 160 h for XRD analysis (Rigaku UltimaIV; CuKα 40 mA, 40 kV, Tokyo, Japan). All of the experiments were conducted in duplicate.

2.3. Zeta-Potential Measurement

Ac. aromatica cells were harvested, washed twice, and re-suspended in 10 mL of 10 mM NaCl solution (pH 2.5 with HCl or NaOH) to a final cell density of 10^8 cells/mL. After the addition of Au(III) at 10 mg/L, cells were left for 30 min prior to the zeta-potential measurement (Malvern ZETASIZER Nano series, Malvern Co., Ltd., Malvern, UK). The measurement was conducted in duplicate.

2.4. Ultra-Thin Section Transmission Electron Microscopy (TEM) Observation

TEM ultra-thin section was performed to observe the distribution and localization of the resultant bio-AuNPs. Cells were collected at 160 h after exposure to Au(III) by centrifugation (12,000 rpm for 10 min), followed by a two-step cell fixation (by using mixture of 4% paraformaldehyde plus 2.5% glutaraldehyde, followed by 1% osmium tetroxide). Cells were dehydrated using an ethanol series (70%, 80%, 90% and 99.5% ethanol for 5 min each step, and finally 100% dried ethanol for 10 min), washed with propylene oxide and finally polymerized with resin (contained Epon 812, DDSA, NMA, and DMP-30). The polymerized samples were cut into 70 nm thickness with a diamond knife (SUMI knife) using ultramicrotome (Leica EM UC7). The ultra-thin film was located on the copper micro grid and stained with ESTM and Pb-citrate for 10 min, respectively, prior to TEM observation (FEI TECNAI-20, Hillsboro, OR, USA). TEM images were used to calculate the average density of bio-AuNPs (particles/cell) under each condition.

2.5. Particle Size Analysis Using Image-J

Image-J software (National Institute of Health, Rockville, MD, USA) was used to analyze the particle size of bio-AuNPs. A total of over 70 nanoparticles were analyzed to calculate the diameter and its standard deviation (except that only 25 and 17 particles were available at 0 and 5 mM formate, respectively). Firstly, the images were calibrated and thresholded by selecting the ROI (region of interest) and removing the background noise. The particles were then analyzed with the "Analyze Particle" function, which calculates the projected area of an individual particle. Assuming that the particle is spherical, the diameter of each particle was calculated from its projected area.

3. Results and Discussion

3.1. Au(III) Biosorption and Bioreduction

About 8.5–9 mg/L of Au(III) ions were rapidly biosorped onto the *Ac. aromatica* cell surface within 10 min, before adding formate as e-donor at 1 h (Figure 1). In fact, the zeta-potential measurement showed that a weakly positive surface charge exhibited by *Ac. aromatica* cells (+2.5 mV at pH 2.5) was shifted slightly negative (+1.9 mV at pH 2.5) after mixing with Au(III) (in the form of $Au^{III}Cl_4^-$) (Figure 2), implying the occurrence of Au(III) biosorption on the cell surface. On the other hand,

no instant decrease in Au concentration was observed in cell-free controls (Figure 1a). Upon the addition of formate at 1 h, the initial biosorption step was followed by an apparent induction phase before Au(III) bioreduction was started to produce Au(0) (Figure 1b). Higher formate concentrations led to less noticeable induction time and faster Au(III) bioreduction: At 1, 5, 10, and 20 mM formate, Au(III) was completely reduced within 60, 60, 50, and 40 h, respectively (Figure 1b). Meanwhile, in cell-free controls, the Au concentration started to decrease only after 40 h due to its chemical reduction by 20 mM formate (Figure 1a). Without formate addition, the biosorption step was followed by a slower and incomplete decrease in the Au concentration (Figure 1b). Addition of 5 mM Cu^{2+} simultaneously with 20 mM formate at 1 h did not show a significantly different trend in soluble Au concentrations, when compared to that without Cu^{2+} (Figure 1b).

As compared to the case with *At. thiooxidans* [33], it was possible to rapidly produce bio-AuNPs by using *Ac. aromatica* with addition of formate as e-donor. Also, the fact that biomass of acidophilic heterotrophs is generally more readily obtained compared to the autotrophs suggest the potential advantage of using acidophilic heterotrophs for bio-AuNPs from acidic solutions.
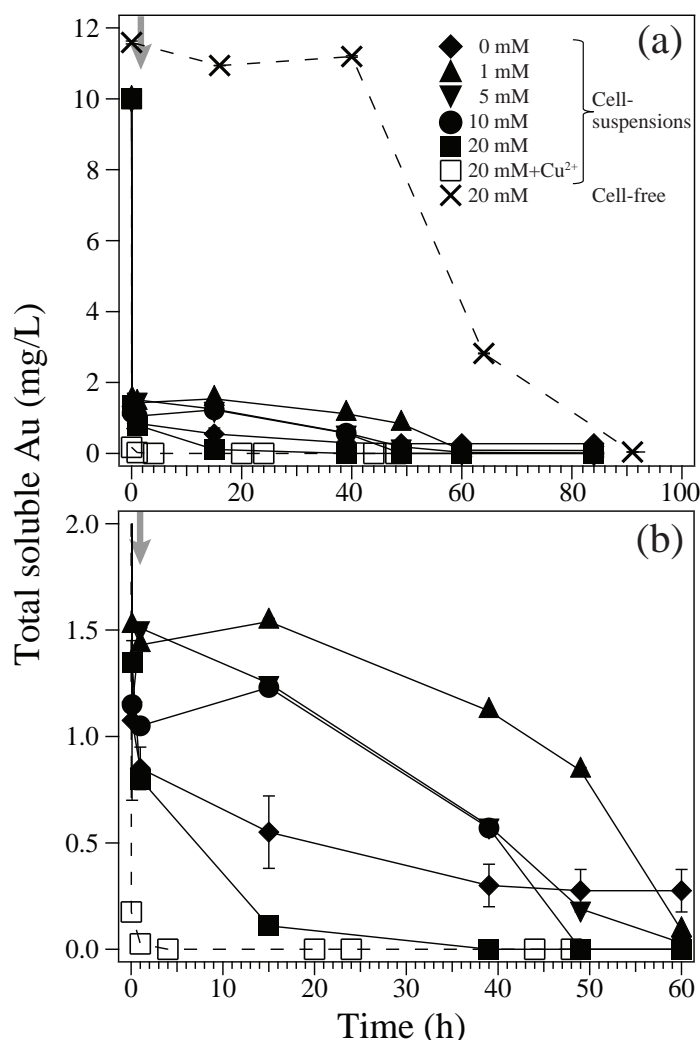

Figure 1. Au(III) biosorption and bioreduction in cell-suspensions of *Ac. aromatica* (pH 2.5). (**a**) Different initial concentrations of formate were used as e-donor; ◆ 0 mM, ▲ 1 mM, ▼5 mM, ●10 mM, and ■ 20 mM (solid lines). As a potential enzymatic inhibitor, 5 mM Cu^{2+} was added with 20 mM formate (□; dotted line). Cell-free controls with 20 mM formate (×; dotted line) were also tested. (**b**) shows the same data on an enlarged *x* and *y*-axis. Grey arrows indicate the time of formate addition at 1 h.
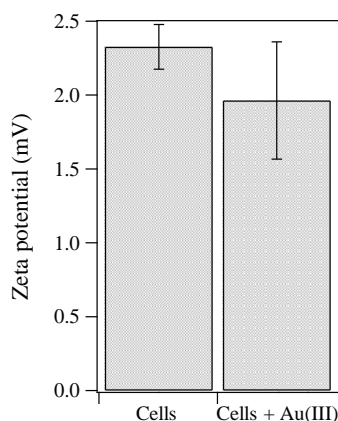
Figure 2. Zeta-potential measurement of *Ac. aromatica* cells at pH 2.5, with or without mixing with 10 mg/L Au(III).

3.2. Size, Density and Localization of Bio-AuNPs

3.2.1. Size and Density

After Au(III) reduction to produce bio-AuNPs, as confirmed by XRD analysis (Figure 3), *Ac. aromatica* cell-suspensions exhibited different intensity of pink color, in accordance with the initial formate concentration (Figure 4b–f), except at 0 mM formate where Au(III) bioreduction was incomplete and no clear color change was noticed (Figure 4a). TEM observation (Figure 5) combined with Image-J particle size analysis (Figure 6) revealed that Au(III) bioreduction at increasing formate concentrations (1, 5, 10, 20 mM) resulted in higher bio-AuNPs densities (2.3, 17, 62, and 97 particles/cell; Figure 5b–e), with finer particle sizes (48, 24, 13, and 12 nm; Figure 6b–e), respectively. The addition of Cu^{2+}, together with 20 mM formate, led to the production of significantly fewer but larger particles (6.5 particles/cell and 26 nm; Figures 5f and 6f, respectively) as compared to the Cu^{2+}-free counterpart (97 particles/cell and 12 nm; Figures 5e and 6e, respectively). Slightly purple coloration in cell-free controls with 20 mM formate (Figure 3g), together with a decrease in total Au concentration (Figure 1a), suggested the formation of relatively larger bio-AuNPs. However, it was not possible to harvest any precipitates from the solution by centrifugation. The above results indicate that the color transition from light-purple, pink, then to pink-red (Figure 4b–f) was particle-size dependent (arranged roughly from larger to smaller particle size; Figure 6b–f). Indeed, color change of several types of biomass after exposure to Au(III) ions was also reported in previous studies, e.g., [25–27,35]. Purple-pink coloration of colloidal Au is due to excitation of surface plasmon vibrations in the AuNPs [36]. Use of heat-killed *Ac. aromatica* cells instead of active cells generally resulted in the production of fewer and larger bio-AuNPs (data not shown). This indicated the importance of using active cells for bionanoparticles production, as was also the case in bio-PdNPs formation [13].
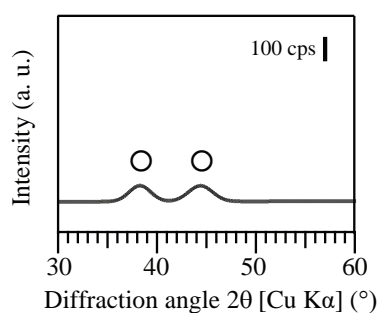

Figure 3. X-ray diffraction pattern of the resultant Au(0) bionanoparticles produced by *Ac. aromatica* using 20 mM formate as e-donor. Open circles are assigned to metallic Au(0) (PDF No. 03-065-8601).
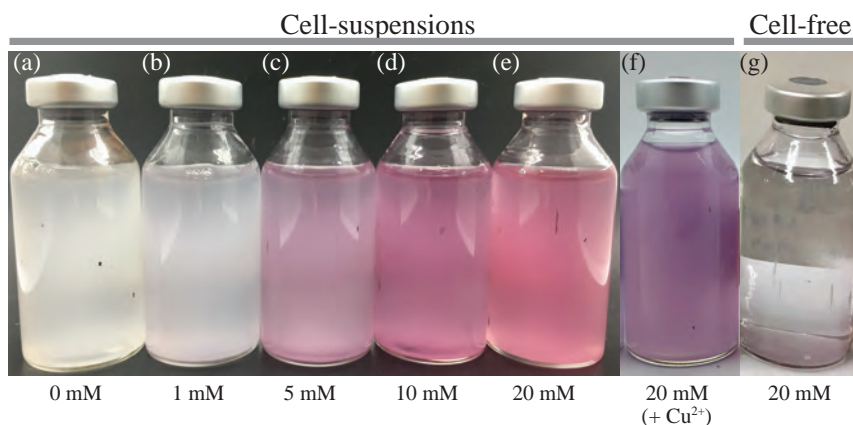
Figure 4. Color change of *Ac. aromatica* cell-suspensions after Au(III) reduction (at 160 h after exposure to 10 mg/L Au(III)). Formate was added as e-donor at; (**a**) 0 mM, (**b**) 1 mM, (**c**) 5 mM, (**d**) 10 mM, or (**e**) 20 mM. (**f**) As a possible enzymatic inhibitor, 5 mM Cu^{2+} was simultaneously added together with 20 mM formate. (**g**) Cell-free controls were also tested at 20 mM formate.
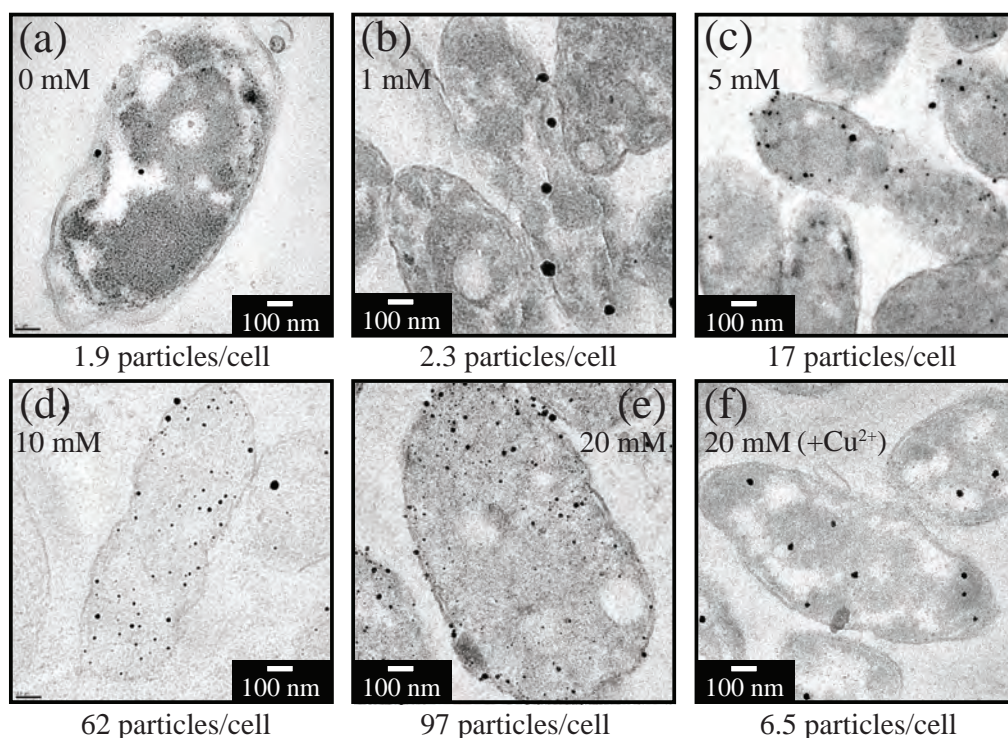

Figure 5. Ultra-thin section TEM images of *Ac. aromatica* cells collected at 160 h after exposure to 10 mg/L Au(III). Formate was added as e-donor at; (**a**) 0 mM, (**b**) 1 mM, (**c**) 5 mM, (**d**) 10 mM, or (**e**) 20 mM. (**f**) As a possible enzymatic inhibitor, 5 mM Cu^{2+} was simultaneously added together with 20 mM formate. Densities of Au(0) bionanoparticles (NPs/cell) were calculated and indicated underneath respective TEM images. The total number of particles counted were as follows: (**a**) $n = 25$ (in 13 cells); (**b**) $n = 18$ (in 8 cells); (**c**) $n = 119$ (in 7 cells); (**d**) $n = 493$ (in 8 cells); (**e**) $n = 681$ (in 7 cells); and, (**f**) $n = 71$ (in 11 cells).
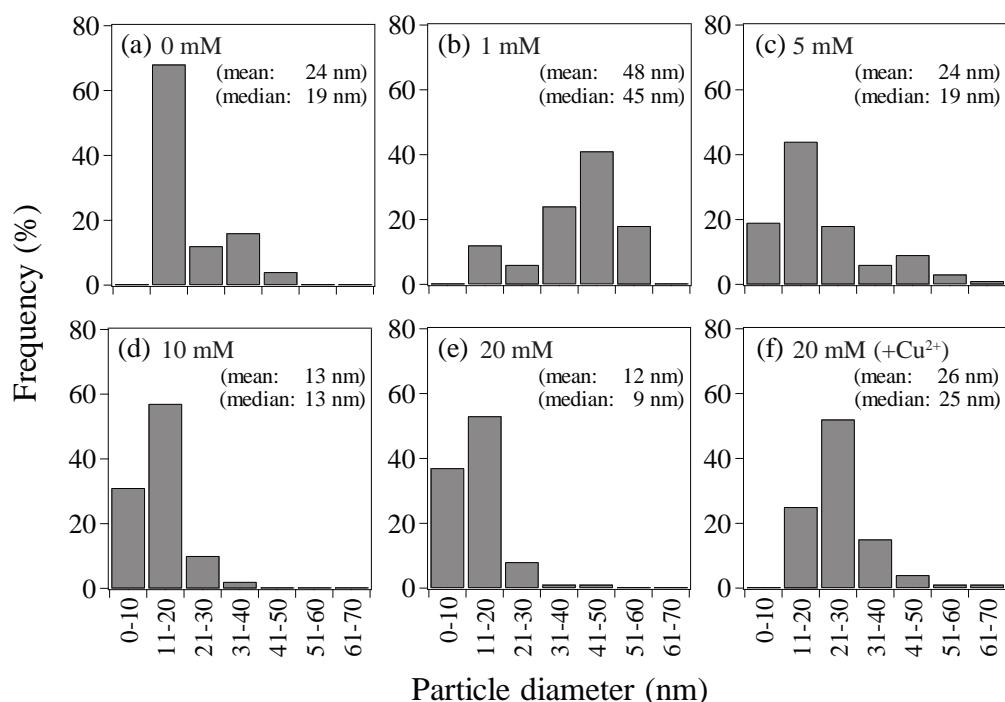
Figure 6. Particle size distribution of Au(0) bionanoparticles produced by *Ac. aromatica* at initial formate concentrations of; (**a**) 0 mM (cf., Figure 5a, *n* = 25), (**b**) 1 mM (cf., Figure 5b, *n* = 18), (**c**) 5 mM (cf., Figure 5c, *n* = 119), (**d**) 10 mM (cf., Figure 5d, *n* = 493), (**e**) 20 mM (cf., Figure 5e, *n* = 681) or (**f**) 20 mM + Cu^{2+} (cf., Figure 5f, *n* = 71).

3.2.2. Localization

According to TEM images, bio-AuNPs were formed intracellularly (both in the periplasmic space and inside cytoplasm; Figure 5a–f). In the case of Pd(0) bionanoparticles (bio-PdNPs) production by *Ac. aromatica*, addition of Cu^{2+} strongly inhibited initial enzymatic Pd(0) nucleation, forming only a few, much larger triangle and penta-/hexagonal Pd(0) particles [13]. Since a similar observation was found with bio-AuNPs formation (as described in Section 3.2.1), it may be possible that a common mechanism is shared between Pd(0) and Au(0) bionanoparticles formation by *Ac. aromatica* and that addition of Cu^{2+} deactivates most of its responsible enzymatic, as well as "metal trafficking", protein activities.

3.3. Schematic Summary of Bio-AuNPs Production by Ac. Aromatica

Based on the results obtained above, the schematic flow of bio-AuNPs formation by *Ac. aromatica* is proposed as shown in Figure 7.

In some studies, the use of H_2 (but not organic acids such as lactate) was essential to support Au(III) reduction [25,26], and the involvement of hydrogenase(s) was suggested in *S. algae* [25], *E. coli* and *D. desulfuricans* [24]. In this study, formate played a role as an effective e-donor. Here, sodium formate (HCOONa) added to cell-suspensions as e-donor exists mostly in the form of formic acid (HCOOH; pKa = 3.8) under acidic pHs (pH 2.5 in this study). Formic acid can diffuse through the cell membrane to deprotonate to cause acidification of the cytoplasm (Equation (1)) [37]. Since the presence of putative formate dehydrogenase (FDH) enzyme is predicted from the genome sequence of *Acidocella* sp. (e.g., *Ac. aminolytica* DSM 11237; *Acidocella* sp. MX-AZ02) [13], formic acid diffused into the cytoplasm can be decomposed by FDH to release H_2 gas (Equation (2)) to act as a reducing agent for Au(0) nucleation.

$$HCOOH \rightleftharpoons HCOO^- + H^+ \tag{1}$$

$$HCOOH \rightarrow CO_2 + H_2 \tag{2}$$

When formate decomposition (Equation (2)) is chemically facilitated (e.g., by catalytic activity of Pd(0); [38]), the resultant H_2 gas can readily act as a chemical reducing agent both in extracellular and intracellular (by diffusion through the cell membrane) regions: In fact, when *Ac. aromatica* was tested for bio-PdNPs production, the addition of a smaller amount of formate (i.e., 5 mM) was sufficient to reduce 100 mg/L Pd(II) to produce finer, intracellular, and periplasmic bio-PdNPs, whereas increasing the formate concentration led to the formation of extracellular Pd(0) aggregates [13]. This effect was also likely further facilitated by the self-catalytic activity of H_2-absorbing Pd(0).
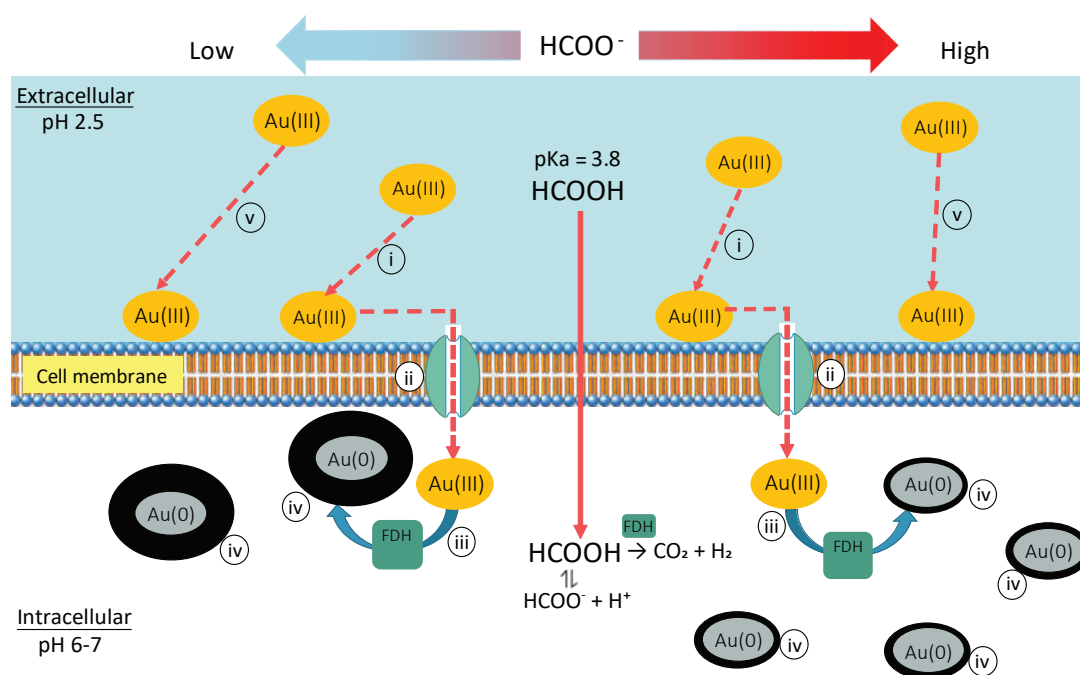

Figure 7. Proposed mechanism of bio-AuNPs production by *Ac. aromatica*: (**i**) Au(III) ions (in the form of $AuCl_4{}^-$) are adsorbed onto the slightly positively charged cell surface. (**ii**) Au(III) ions are transported into cytoplasm via membrane "Au(III) trafficking" proteins. (**iii**) Au(III) ions are reduced to form Au(0) nuclei via intracellular enzymatic reaction (possibly FDH) to decompose formate to produce H_2 as a reducing force (**iv**) At lower formate concentrations fewer Au(0) nucleation sites appear leading to greater crystal growth for individual particles, whereas at higher formate concentrations the number of Au(0) nuclei is increased leading to smaller crystal growth for individual particles. (**v**) As the flow from (**i**) to (**iv**) proceeds, remaining Au(III) ions left in the bulk solution can sequentially adsorb on the cell surface by occupying a vacancy created upon trafficking of the former adsorbate into the cytoplasm, to further proceed to (**ii**).

In the case of Au, on contrary to that of Pd [13], addition of an increasing amount of formate corresponded to formation of finer, intracellular and periplasmic bio-AuNPs with a higher density. This was likely because formate decomposition to produce H_2 as reducing force mainly occurred as intracellular enzymatic reaction (supposedly FDH) (Figure 7). Accordingly, the use of a greater amount of formate led to the activation of more enzymatic reaction sites (i.e., occurrence of more Au(0) nucleation loci), and thus a faster Au(III) bioreduction speed (Figure 1). Formation of fewer number of Au(0) nuclei at lower formate concentrations generally led to greater crystal growth (Figures 4, 6 and 7).

In most of the previous studies, no external e-donor was added to facilitate Au reduction, in other words, the reaction relied on intracellular electron carriers (such as NADH) accumulated during pre-growth (so as the case with 0 mM formate addition in this study). Only a few studies used external e-donors, such as H_2 [24–26] and lactate [28]. In any case, the size-control of bio-AuNPs by means of external e-donor had not yet been evaluated in detail. Thus, the results obtained here first

demonstrated the possibility of size-controlled bacterial bio-AuNPs production by manipulating the e-donor concentration, combined with the use of an enzyme inhibitor.

4. Conclusions

- The acidophilic Fe(III)-reducing heterotrophic bacterium, *Acidocella aromatica* PFBC was successfully used for intracellular gold recovery as bio-AuNPs from highly acidic Au(III) solutions via a simple one-step reaction.

- Use of increasing concentration of formate (as e-donor) corresponded to a greater number of Au(0) nucleation sites with less crystal growth: At 1, 5, 10, or 20 mM formate, bio-AuNPs of 48, 24, 13, or 12 nm, with 2.3, 17, 62, or 97 particles/cell, respectively, were produced.

- The presence of Cu^{2+} was inhibitory to intracellular enzymatic reaction, resulting in significantly fewer Au(0) nucleation, but in enhanced crystal growth.

- It was possible to control the size of bio-AuNPs by modifying the e-donor concentration combined with a use of enzyme inhibitor: bio-AuNPs of 48 nm, 26 nm, or 13 nm (nearly within normal distribution) was produced by use of 1 mM formate, 20 mM formate (+Cu^{2+}), or 10 mM formate, respectively.

- The knowledge obtained from this fundamental study is expected to be applied to the actual acidic Au leachate from "urban mine" resources such as Au-bearing printed circuit boards (PCBs).

Author Contributions: Intan Nurul Rizki performed the experiments and prepared the manuscript draft under the supervision of Naoko Okibe.

References

1. Bernstein, P.L.; Volcker, P.A. *The Power of Gold: The History of an Obsession*; John Wiley & Sons: Hoboken, NJ, USA, 2012.

2. Sperling, R.A.; Gil, P.R.; Zhang, F.; Zanella, M.; Parak, W.J. Biological applications of gold nanoparticles. *Chem. Soc. Rev.* **2008**, *37*, 1896–1908. [CrossRef] [PubMed]

3. Chen, P.C.; Mwakwari, S.C.; Oyelere, A.K. Gold nanoparticles: From nanomedicine to nanosensing. *Nanotechnol. Sci. Appl.* **2008**, *1*, 45. [PubMed]

4. Das, S.K.; Das, A.R.; Guha, A.K. Gold nanoparticles: Microbial synthesis and application in water hygiene management. *Langmuir* **2009**, *25*, 8192–8199. [CrossRef] [PubMed]

5. Dahl, J.A.; Maddux, B.L.; Hutchison, J.E. Toward greener nanosynthesis. *Chem. Rev.* **2007**, *107*, 2228–2269. [CrossRef] [PubMed]

6. Herzing, A.A.; Kiely, C.J.; Carley, A.F.; Landon, P.; Hutchings, G.J. Identification of active gold nanoclusters on iron oxide supports for co oxidation. *Science* **2008**, *321*, 1331–1335. [CrossRef] [PubMed]

7. Verma, M.L. Nanobiotechnology advances in enzymatic biosensors for the agri-food industry. *Environ. Chem. Lett.* **2017**, *15*, 555–560. [CrossRef]

8. Verma, M.L. Enzymatic nanobiosensors in the agricultural and food industry. In *Nanoscience in Food and Agriculture 4*; Wiley: Hoboken, NJ, USA, 2017; pp. 229–245.

9. Lee, J.-S.; Cho, J.; Lee, C.; Kim, I.; Park, J.; Kim, Y.-M.; Shin, H.; Lee, J.; Caruso, F. Layer-by-layer assembled charge-trap memory devices with adjustable electronic properties. *Nat. Nanotechnol.* **2007**, *2*, 790–795. [CrossRef] [PubMed]

10. Zhao, P.; Li, N.; Astruc, D. State of the art in gold nanoparticle synthesis. *Coord. Chem. Rev.* **2013**, *257*, 638–665. [CrossRef]

11. Rai, M.; Yadav, A.; Gade, A. CRC 675—Current trends in phytosynthesis of metal nanoparticles. *Crit. Rev. Biotechnol.* **2008**, *28*, 277–284. [CrossRef] [PubMed]

12. Mohanpuria, P.; Rana, N.K.; Yadav, S.K. Biosynthesis of nanoparticles: Technological concepts and future applications. *J. Nanopart. Res.* **2008**, *10*, 507–517. [CrossRef]

13. Okibe, N.; Nakayama, D.; Matsumoto, T. Palladium bionanoparticles production from acidic Pd(II) solutions and spent catalyst leachate using acidophilic Fe(III)-reducing bacteria. *Extremophiles* **2017**, *21*, 1091–1100. [CrossRef] [PubMed]

14. Ehrlich, H.L.; Newman, D.K.; Kappler, A. *Ehrlich's Geomicrobiology*, 6th ed.; CRC Press: Boca Raton, FL, USA, 2015.

15. Korobushkina, E.; Korobushkin, I. The interaction of gold with bacteria and the formation of new gold. *Doklady Akademii Nauk SSSR* **1986**, *287*, 978.

16. Southam, G.; Beveridge, T.J. The in vitro formation of placer gold by bacteria. *Geochim. Cosmochim. Acta* **1994**, *58*, 4527–4530. [CrossRef]

17. Southam, G.; Beveridge, T.J. The occurrence of sulfur and phosphorus within bacterially derived crystalline and pseudocrystalline octahedral gold formed in vitro. *Geochim. Cosmochim. Acta* **1996**, *60*, 4369–4376. [CrossRef]

18. Kalishwaralal, K.; Deepak, V.; Pandian, S.R.K.; Gurunathan, S. Biological synthesis of gold nanocubes from bacillus licheniformis. *Bioresour. Technol.* **2009**, *100*, 5356–5358. [CrossRef] [PubMed]

19. Wen, L.; Lin, Z.; Gu, P.; Zhou, J.; Yao, B.; Chen, G.; Fu, J. Extracellular biosynthesis of monodispersed gold nanoparticles by a SAM capping route. *J. Nanopart. Res.* **2009**, *11*, 279–288. [CrossRef]

20. Li, Y.; Li, Y.; Li, Q.; Fan, X.; Gao, J.; Luo, Y. Rapid biosynthesis of gold nanoparticles by the extracellular secretion of bacillus niabensis 45: Characterization and antibiofilm activity. *J. Chem.* **2016**, *2016*, 7. [CrossRef]

21. Markus, J.; Mathiyalagan, R.; Kim, Y.-J.; Abbai, R.; Singh, P.; Ahn, S.; Perez, Z.E.J.; Hurh, J.; Yang, D.C. Intracellular synthesis of gold nanoparticles with antioxidant activity by probiotic lactobacillus kimchicus DCY51^T isolated from Korean kimchi. *Enzyme Microb. Technol.* **2016**, *95*, 85–93. [CrossRef] [PubMed]

22. Nair, B.; Pradeep, T. Coalescence of nanoclusters and formation of submicron crystallites assisted by lactobacillus strains. *Cryst. Growth Des.* **2002**, *2*, 293–298. [CrossRef]

23. Husseiny, M.; El-Aziz, M.A.; Badr, Y.; Mahmoud, M. Biosynthesis of gold nanoparticles using Pseudomonas aeruginosa. *Spectrochim. Acta Part A Mol. Biomol. Spectrosc.* **2007**, *67*, 1003–1006. [CrossRef] [PubMed]

24. Deplanche, K.; Macaskie, L. Biorecovery of gold by *Escherichia coli* and *Desulfovibrio desulfuricans*. *Biotechnol. Bioeng.* **2008**, *99*, 1055–1064. [CrossRef] [PubMed]

25. Kashefi, K.; Tor, J.M.; Nevin, K.P.; Lovley, D.R. Reductive precipitation of gold by dissimilatory Fe(III)-reducing *Bacteria* and *Archaea*. *Appl. Environ. Microbiol.* **2001**, *67*, 3275–3279. [CrossRef] [PubMed]

26. Konishi, Y.; Tsukiyama, T.; Ohno, K.; Saitoh, N.; Nomura, T.; Nagamine, S. Intracellular recovery of gold by microbial reduction of AuCl$_4$$^-$ ions using the anaerobic bacterium *Shewanella algae*. *Hydrometallurgy* **2006**, *81*, 24–29. [CrossRef]

27. He, S.; Guo, Z.; Zhang, Y.; Zhang, S.; Wang, J.; Gu, N. Biosynthesis of gold nanoparticles using the bacteria *Rhodopseudomonas capsulata*. *Mater. Lett.* **2007**, *61*, 3984–3987. [CrossRef]

28. Feng, Y.; Lin, X.; Wang, Y.; Wang, Y.; Hua, J. Diversity of aurum bioreduction by *Rhodobacter capsulatus*. *Mater. Lett.* **2008**, *62*, 4299–4302. [CrossRef]

29. Nangia, Y.; Wangoo, N.; Sharma, S.; Wu, J.; Dravid, V.; Shekhawat, G.S.; Suri, C.R. Facile biosynthesis of phosphate capped gold nanoparticles by a bacterial isolate *Stenotrophomonas maltophilia*. *Appl. Phys. Lett.* **2009**, *94*, 233901-1–233901-3. [CrossRef]

30. Reith, F.; Rogers, S.L.; McPhail, D.; Webb, D. Biomineralization of gold: Biofilms on bacterioform gold. *Science* **2006**, *313*, 233–236. [CrossRef] [PubMed]

31. Lengke, M.; Southam, G. Bioaccumulation of gold by sulfate-reducing bacteria cultured in the presence of gold(I)-thiosulfate complex. *Geochim. Cosmochim. Acta* **2006**, *70*, 3646–3661. [CrossRef]

32. Li, J.; Li, Q.; Ma, X.; Tian, B.; Li, T.; Yu, J.; Dai, S.; Weng, Y.; Hua, Y. Biosynthesis of gold nanoparticles by the extreme bacterium *Deinococcus radiodurans* and an evaluation of their antibacterial properties. *Int. J. Nanomed.* **2016**, *11*, 5931–5944. [CrossRef] [PubMed]

33. Lengke, M.F.; Southam, G. The effect of thiosulfate-oxidizing bacteria on the stability of the gold-thiosulfate complex. *Geochim. Cosmochim. Acta* **2005**, *69*, 3759–3772. [CrossRef]

34. Jones, R.M.; Hedrich, S.; Johnson, D.B. *Acidocella aromatica* sp. nov.: An acidophilic heterotrophic alphaproteobacterium with unusual phenotypic traits. *Extremophiles* **2013**, *17*, 841–850. [CrossRef] [PubMed]

35. Liz-Marzán, L.M. Nanometals: Formation and color. *Mater. Today* **2004**, *7*, 26–31. [CrossRef]

36. Mulvaney, P. Surface plasmon spectroscopy of nanosized metal particles. *Langmuir* **1996**, *12*, 788–800. [CrossRef]

37. Baker-Austin, C.; Dopson, M. Life in acid: pH homeostasis in acidophiles. *Trends Microbiol.* **2007**, *15*, 165–171. [CrossRef] [PubMed]

38. Hill, S.P.; Winterbottom, J.M. The conversion of polysaccharides to hydrogen gas. Part 1: The palladium catalysed decomposition of formic acid/sodium formate solutions. *J. Technol. Biotechnol.* **1988**, *41*, 121–133. [CrossRef]